Eur. Phys. J. D **45**, 99–106 (2007)
DOI: 10.1140/epjd/e2007-00198-1

THE EUROPEAN PHYSICAL JOURNAL D

Towards optical spectroscopy of the element nobelium (Z = 102) in a buffer gas cell

First on-line experiments on ^{155}Yb at the velocity filter SHIP with a novel ion collection and atom re-evaporation method of high efficiency

H. Backe[1], P. Kunz[1,a], W. Lauth[1], A. Dretzke[1], R. Horn[1], T. Kolb[1], M. Laatiaoui[2], M. Sewtz[2], D. Ackermann[3], M. Block[3], F. Herfurth[3], F.P. Heßberger[3], S. Hofmann[3], and R. Mann[3]

[1] Institut für Kernphysik der Universität Mainz, 55099 Mainz, Germany
[2] Department für Physik, Ludwig-Maximilians-Universität München, 85748 Garching, Germany
[3] Gesellschaft für Schwerionenforschung, 64291 Darmstadt, Germany

Received 18 January 2007 / Received in final form 11 April 2007
Published online 20 June 2007

Abstract. For the investigation of the atomic level structure of heavy elements which can only be produced at on-line facilities such as GSI, a novel experimental procedure has been developed. It is based on Radiation Detected Resonance Ionization Spectroscopy (RADRIS) and can be applied to elements like nobelium produced at rates of a few ions per second. Fusion reaction products are separated from the primary beam by the velocity filter SHIP at GSI, stopped in a buffer gas cell, collected on a tantalum filament and then re-evaporated as atoms. The ions produced by resonance ionization with tunable laser beams are detected via their characteristic α decay. First on-line experiments on α-active ^{155}Yb, which is supposed to have an atomic level structure similar to nobelium, were performed. These test experiments focused on the optimization of the collection and re-evaporation process of the radioactive ions, the laser ionization efficiency and the detection via α decay. An overall efficiency for RADRIS of 0.8% with respect to the target production rate was measured. While further improvements of this efficiency are in progress it should already be sufficient for the search for atomic levels in nobelium.

PACS. 31.10.+z Theory of electronic structure, electronic transitions, and chemical binding – 32.80.Rm Multiphoton ionization and excitation to highly excited states – 32.30.-r Atomic spectra – 27.90.+b $220 \leq A$

1 Introduction

Some of the most fascinating studies of the heaviest actinides and the transactinides concern the influence of increasingly strong relativistic effects on the valence-electron configuration of the atom and its consequences on their chemical behavior. At present the most advanced method for studying trans-einsteinium elements is the aqueous phase and gas phase chemistry of single atoms [1–4]. These techniques have already provided detailed chemical information for elements up to the nuclear charge number $Z = 108$ [5], and very recently $Z = 112$ [6]. The aim of such experiments is to compare the chemical properties within a group of homolog elements. Relativistic effects gain importance for the heaviest elements in the region of $Z = 100$ so that simple extrapolation of systematics, e.g. the oxidation states, electron affinity, and complex formation, may not lead to reliable predictions. These relativistic effects on the valence electrons are mainly due to the shrinking of the wave functions of s- and $p_{1/2}$-electrons and a change of the shielding of the nuclear potential by s- and $p_{1/2}$-inner shell electrons. In the case of heavy actinides and trans-actinides the valence electrons are occupying the $5f$-, $6d$-, $7p$- and $7s$-orbitals. Due to their different radial charge distributions such relativistic effects have a grave influence on binding energies of corresponding electron configurations and therefore as well on the chemical properties of these elements. Relativistic quantum chemical atomic and molecular codes allow for predictions and descriptions of atomic and molecular properties [7].

An even more critical test of relativistic effects would be to compare atomic properties, such as the first

[a] e-mail: pkunz@uni-mainz.de

ionization potential and the atomic level schemes, with modern Multi-Configuration-Dirac-Fock (MCDF) or Coupled-Cluster calculations and other methods [8–10]. However, the required experimental methods have to be sensitive enough to explore atomic (and perhaps also nuclear) properties of trans-einsteinium elements even at very low production rates, short lifetimes and the complete lack of information on atomic excitation schemes. Our experimental approach is based on the Radiation Detected Resonance Ionization Spectroscopy (RADRIS) technique [11]. The method is sensitive enough to be applied to radioactive nuclides with short half-lives (>1ms) and very low production rates (≈10/s) as demonstrated with the hyperfine spectroscopy of ^{240f,242f,244f}Am fission isomers [12,13].

The feasibility of atomic spectroscopy of an element with an unknown level scheme has first been demonstrated on the example of fermium ($Z = 100$) [14]. In this experiment the Ion-Guide detected Resonance Ionization Spectroscopy (IGRIS) method [15] has been employed. This laser spectroscopic method is especially suitable for radionuclides with long half-lives because the probed elements are identified independently of decay times with a quadrupole mass spectrometer. With a total sample amount of less than 4 ng of the isotope ^{255}Fm with a half-life of 20.1 h previously unknown atomic levels were found, transition rates were determined and the hyperfine structure of two optical transitions was investigated [16].

In a research program with the aim to extend these experiments to heavier elements we proposed to investigate the element nobelium ($Z = 102$) at the velocity filter SHIP at GSI. It includes the search for so far totally unknown atomic energy levels and, if this is successful, possibly the determination of the ionization potential. The isotope ^{254}No ($t_{1/2} = 55$ s) can be produced by the fusion reaction ^{208}Pb(^{48}Ca, $2n$)^{254}No with a production cross section of $\sigma = \sim 2$ μb at a projectile energy of 216 MeV [17]. As an α emitter with a relatively short half-life, ^{254}No can be investigated by the RADRIS method which had to be improved and modified to accommodate the prerequisites at SHIP.

Since the target production rate of ^{254}No is only in the order of ≈17 ions/s, and also because the beam isotope ^{48}Ca is extremely expensive, the experimental method for on-line experiments at SHIP was developed on lanthanide elements like erbium and ytterbium on which we report in this contribution. In Section 2 the experimental setup is outlined in general terms. Specific experimental conditions, individual experiments and their results are described in Sections 3 to 5. An outlook in Section 6 discusses the prerequisites and the measurement procedure for on-line spectroscopy on nobelium.

2 Experimental

The experimental setup for on-line RADRIS is shown in Figure 1. The separated fusion product beam from SHIP is stopped in a buffer gas cell with an argon atmosphere of 50–200 mbar. Earlier experiments on americium [18] revealed, that only ≈15% of the beam is neutralized while

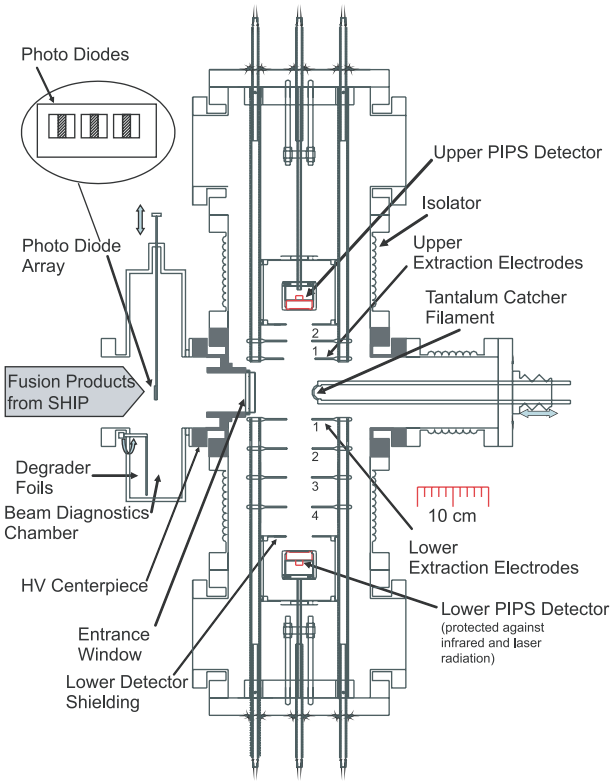

Fig. 1. Optical buffer gas cell for RIS on a fusion product beam from SHIP. The high vacuum of the SHIP beamline and the buffer gas volume are separated by a thin *Mylar* entrance window. The lower PIPS detector is further removed from the center of the cell by two more ring electrodes. This results in a smaller opening angle and thus a lower background from neutrals decaying in the stopping volume.

the rest is stopped as ions. The larger fraction of ions is transported by suitable electrical fields onto an auxiliary electrode, i.e. catcher filament, which must not be seen directly by the particle detectors. The remaining atoms in the stopping volume can be resonantly ionized with laser beams in a fusion product beam-off period. The ions are guided by electrical fields onto the particle detector (Passivated Implanted Planar Silicon semiconductor detector, PIPS) with which the resonance ionization is identified by the α decay.

As depicted schematically in Figure 1, profile and intensity of the incoming fusion product beam from SHIP can be measured with a photo diode array, consisting of three windowless Hamamatsu photo diodes with an active area of 3 mm (horizontal) × 10 mm (vertical), on the high vacuum side of the optical cell. Here, also the beam energy can be reduced with retractable degrader foils if necessary. The beam penetrates a 6 μm thick *Mylar* entrance window with a diameter of 59 mm. The beam energy and the argon buffer gas pressure are adjusted so that the majority of the fusion products is stopped in the center of the cell.

The purity of the argon buffer gas is of high importance for the prevention of unwanted chemical reactions. Therefore, a zirconium getter cartridge and a zirconium

getter pump (SAES) were implemented into the buffer gas inlet system. Additionally, the buffer gas cell was baked out at ≈90 °C. The impurities are monitored with a residual gas analyzer (Balzers). These combined measures ensured that the concentration of gas impurities could be kept below 10^{-6}.

For the first on-line RIS experiments on ^{155}Yb a resonant two-step excitation scheme was provided by two dye lasers (FL2002, Lambda Physik: spectral bandwidth ≈6 GHz) which were pumped simultaneously by either an XeCl excimer laser (LPX210i, Lambda Physik: $\lambda = 308$ nm, $E_{pulse} = 300$ mJ at a maximum repetition rate of 100 Hz), or an XeF excimer laser (EMG104, Lambda Physik: $\lambda = 351/355$ nm, $E_{pulse} = 60$ mJ at a max. repetition rate of 500 Hz). The laser beams were transported in separate optical fibers to the experiment where they were overlapped in the interaction volume of the optical cell.

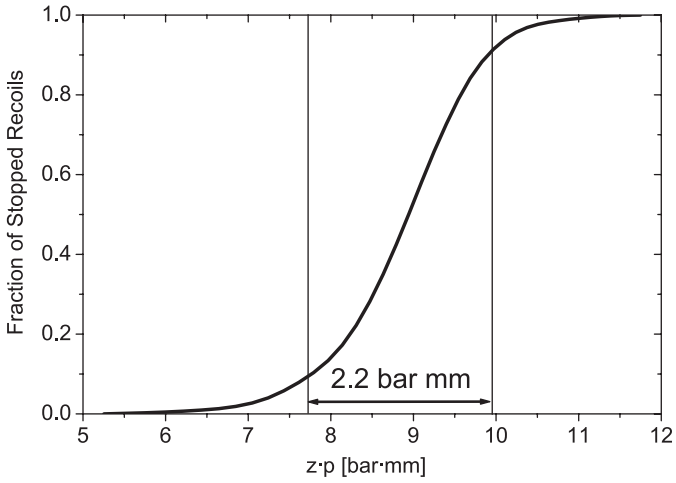

Fig. 2. Fraction of stopped ^{152,153}Er recoils in the buffer gas as a function of distance from the entrance window in beam direction $z \times$ argon gas pressure p.

3 Stopping distribution of the fusion product beam

Several on-line experiments with ^{152,153}Er and ^{155}Yb fusion reaction beams were performed in order to establish a measurement procedure for on-line laser spectroscopy of nobelium. These isotopes were chosen for the purposes of development because their production rates are typically several orders of magnitude higher than for ^{254}No and the atomic levels are well-known. Furthermore, ^{155}Yb is the homologous lanthanide to the actinide ^{254}No. Both isotopes are supposed to have a similar atomic level structure.

A first on-line experiment had the objective to determine the stopping distribution of the fusion product beam in the buffer gas, using the fusion reaction ^{116}Sn(^{40}Ar, xn) ^{152,153}Er with a beam energy of 167 MeV and a target thickness of 0.438 mg/cm^2. The isotopes ^{152,153}Er are α emitters with half-lives $t_{1/2} = 10.3$ s and $t_{1/2} = 37.1$ s, respectively.

The energy and the spatial distribution of the fusion product ions were measured with a silicon strip detector with an active area of 57.5×57.5 mm^2 for different buffer gas pressures and distances from the entrance window in beam direction. The transverse profile was mostly determined by the diameter of the entrance window whereas the stopping distribution in beam direction depended strongly on the buffer gas pressure. From the measurement of several residual fusion product energies a function, depending on the buffer gas pressure and the distance from the entrance window, was derived for the fraction of stopped fusion products, see Figure 2. The result indicates that a stopping efficiency of 90% is reached within 2.2 bar × mm. This translates with the dimensions of the buffer gas cell, so that the fusion product beam is stopped at a distance of less than 10 cm from the entrance window, to a pressure of 50–150 mbar.

Further experiments were performed with the isotope ^{155}Yb which is also an α emitter with a half-life

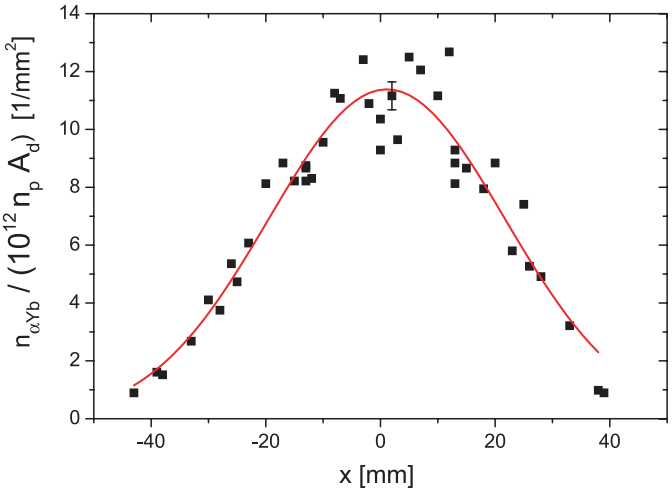

Fig. 3. Horizontal profile of the ^{155}Yb recoil beam. The number of ytterbium α decays $n_{\alpha Yb}$ has been normalized to the number of primary ^{52}Cr beam ions n_p and the detector area A_d. The error bar indicates the standard deviation of a single measurement, the full line a Gaussian fit.

$t_{1/2} = 1.75$ s. The cross section for the fusion reaction ^{107}Ag(^{52}Cr, $p3n$)^{155}Yb is, according to calculations with the statistical evaporation code HIVAP [19], about 15 mb at the chosen ^{52}Cr projectile energy of 237 MeV. With a target of a density-thickness product $\varrho d_{eff} = 0.455$ mg/cm^2 and a beam current of 500 pnA the target production rate amounts to 1.2×10^5/s.

Intensity and profile of the fusion product beam in the horizontal direction were determined with the photo diode array in the high vacuum part of the buffer gas cell, see Figure 1. The α decays of ^{155}Yb were recorded while it was moved on the horizontal plane through the beam. The horizontal profile, displayed in Figure 3, can be approximated well with a Gaussian of amplitude $A_\alpha = 11.5 \times 10^{-12}$/mm^2 and standard deviation $\sigma_x = 20.5$ mm. The vertical profile can also be approximated with a Gaussian of standard

deviation $\sigma_y = 0.7\sigma_x$. With these quantities the number of fusion products which exit SHIP normalized to the number of ^{52}Cr projectiles n_p impinging on the target is given as

$$\frac{n_{\mathrm{Yb}}}{n_p}\epsilon_{SHIP} = \frac{2\pi\sigma_x\sigma_y A_\alpha}{\epsilon_{det}} = 4.3 \times 10^{-8}, \qquad (1)$$

with $\epsilon_{det} = 0.5$ the detection efficiency of the α-particle detector, and n_{Yb} the fusion product number right behind the target. The number of ^{52}Cr projectiles has been determined from a current and time measurement with a Faraday cup, taking into account the charge state 13+ of the ^{52}Cr projectiles, and the beam duty-cycle 5 ms/20 ms. With the transmission efficiency $\epsilon_{SHIP} \approx 0.5$ of SHIP the fusion probability of a projectile with a target nucleus turns out to be $n_{\mathrm{Yb}}/n_p = 8.6 \times 10^{-8}$ from which a fusion cross section $\sigma_{exp} = (n_{\mathrm{Yb}}/n_p)/(\varrho d_{eff} N_A/M_{molar}^{target}) \approx$ 34 mbarn can be estimated. This number is a factor 2.2 larger as the HIVAP calculation mentioned above.

4 The novel ion collection and atom re-evaporation (ICARE) method

Experiments on the direct resonance ionization of the stopped and neutralized fraction of a ^{155}Yb beam lead to a rather low detection efficiency in the order of 10^{-5}. This low number was attributed mainly to the insufficient overlap of the laser beams with the stopping volume which was in this experiment in the order of 60 mm in diameter and 20 mm in depth. A further disadvantage of this direct method is that only the smaller fraction of fusion products which thermalizes in the buffer gas as atoms is used while the larger fraction of ions is discarded, see Section 2. Therefore, a novel method has been developed in which the ions are transported continuously by electrical fields on a small catcher filament opposite to the entrance window, see Figure 1. Here, they are adsorbed and after an appropriate collection time re-evaporated as atoms by a short heating pulse into the buffer gas where they can be resonantly ionized. The advantage of this procedure is, beside that the larger fraction of 85% of ions is utilized, that the interaction region of atoms and laser beams can be kept much smaller in comparison to the direct method.

Figure 1 depicts the position of the tantalum catcher filament in front of the entrance window which was protected with an Al-coated *Mylar* foil of 1.5 μm thickness on the buffer gas side of the optical cell to avoid electrostatic charging and overheating by infrared radiation. The ^{155}Yb ions were stopped between window and filament during an beam-on-period of 2 s and extracted to the filament with an electrical field of ≈100 V/cm field strength.

In order to determine the evaporation temperature of Yb atoms from the filament, a retractable α detector which was installed perpendicular to the beam direction was moved in front of the filament to measure the accumulated activity. After 2.5 s the detector was retracted and the filament was heated up to a temperature of 1400 °C

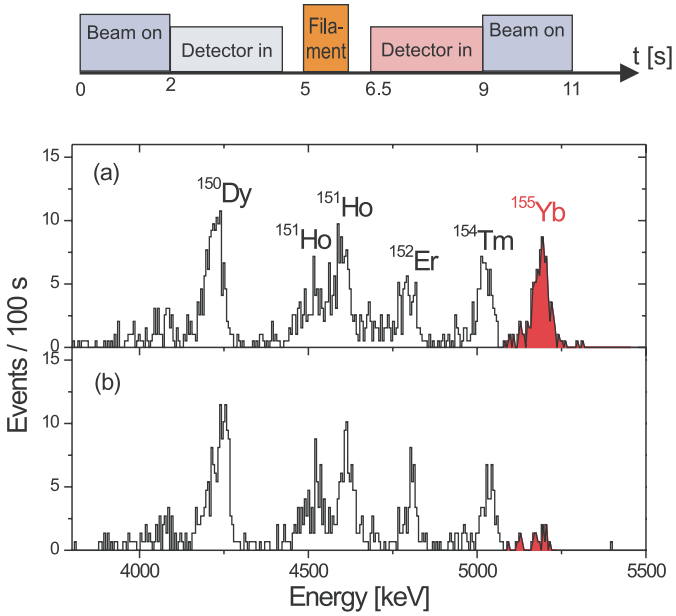

Fig. 4. View graphs demonstrating the evaporation of ^{155}Yb from a tantalum filament at heating. The α-energy spectrum (a), obtained within the measurement sequence shown above, shows the activity of the fusion products on the filament after 6.5 s while the filament was not heated. The α-energy spectrum (b) shows the same except that the filament was heated for a period of 1 s in which it reached a temperature of up to 1400 °C. The remaining α lines are due to long-lived isotopes accumulated on the filament over time.

for 1 s. After the heating period the detector was moved again in front of the filament to measure the α spectrum of the remaining activity. Then the sequence starts again with a beam on period. Figure 4 shows the measurement sequence and two α spectra of the remaining activity after the heating period, one where the filament was heated and one where it was kept at room temperature. The comparison of the ^{155}Yb activities shows clearly that ytterbium is re-evaporated from the filament very efficiently within 1 s at a temperature of 1400 °C. However, it could not be established unambiguously by this method whether the Yb is evaporated in the form of atoms or molecules.

The heating process was also examined in off-line experiments on stable Yb. Instead of the entrance window a sample filament with about 10^{19} atoms of stable Yb was installed into the buffer gas cell. In order to simulate the thermalized ions of the SHIP fusion product beam, Yb atoms were evaporated from the sample filament, resonantly ionized in a two-step excitation scheme with $\lambda_1 = 398.9$ nm, and $\lambda_2 = 399.6$ nm, and collected on the catcher filament. From there Yb atoms were evaporated by heating the filament with a short current pulse and resonantly ionized. The time dependent ion signal was detected with a low noise charge sensitive preamplifier (Canberra Mod. 2004). Evaporation of atoms occurred already at a temperature of 910 °C but for the evaporation of nearly all collected Yb atoms on a time scale of less than 800 ms a temperature of 1300–1400 °C was needed. For the process of ion collection, re-evaporation and

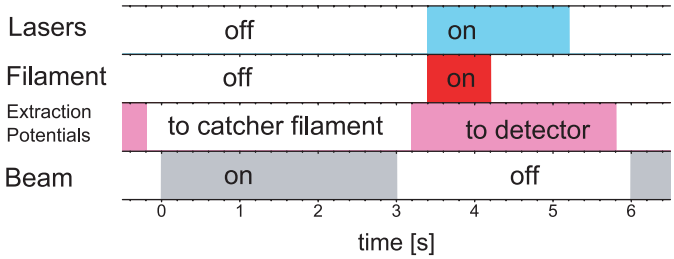

Fig. 5. (Color online) Measurement sequence for RIS on the ionized fraction of the ^{155}Yb fusion product beam, stopped in the buffer gas cell shown in Figure 1.

Table 1. Electrical potentials for the deposition of ionized fusion products on the catcher filament and for their extraction to the lower PIPS detector. The individual components of the ion guide configuration are depicted in Figure 1.

	Extraction potentials for guiding ions to	
	Filament [V]	Detector [V]
Upper Detector	not connected	
Upper Detector Shielding	not connected	
Upper Electrode 2	not connected	
Upper Electrode 1	932	1528
HV Centerpiece	932	1528
Filament	435	1560
Lower Electrode 1	936	1333
Lower Electrode 2	1405	1061
Lower Electrode 3	932	932
Lower Electrode 4	652	652
Lower Detector Shielding	491	491
Lower Detector	0	0

resonance ionization an efficiency in the order of 10^{-2} was determined by comparing the charge of the collected ions with the charge produced by the resonant ionization of the atoms evaporated from the catcher filament.

5 Resonance ionization spectroscopy on ^{155}Yb employing ICARE

For the on-line resonance ionization of ^{155}Yb a periodic measurement sequence, as illustrated in Figure 5, was applied. It was a 6-second-cycle, divided into an accumulation period where the primary beam was switched on for 3 s, and a detection period where the beam was off. During the accumulation period the incoming fusion product ions were guided to the catcher filament by suitable electrical fields. After the beam was turned off the electrical fields were changed so that ions created in the buffer gas close to the filament were transported to the lower α detector. The applied voltages are listed in Table 1. A delay of 200 ms assured that all ions of the fusion product beam were removed from the buffer gas volume prior to the next steps of the sequence. Then the catcher filament, which was made of a tantalum wire of 125 μm diameter in the form of a ring of about 10 mm diameter, was heated by a 200–1000 ms current pulse. The evaporated

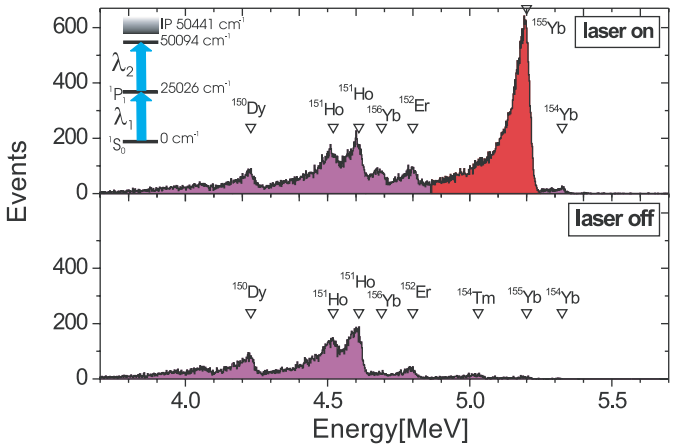

Fig. 6. (Color online) α-energy spectrum of the fusion products with lasers tuned to the excitation scheme for Yb with $\lambda_1 = 398.9$ nm, and $\lambda_2 = 399.6$ nm (laser on) and without laser ionization (laser off).

atoms were ionized by laser beams which were activated at the same time. The laser ions were transported to the detector where their α-energy spectrum was recorded. The resonance ionization was performed with a two-step excitation scheme. The first step with $\lambda_1 = 398.9$ nm populates the $4f^{14}6s6p\ ^1\mathrm{P}_1$ level and the second step with $\lambda_2 = 399.6$ nm leads to a high-lying Rydberg state from which ionization occurs through buffer gas collisions. Typical laser pulse energies were $P_1 = 360\ \mu$J for the first and $P_2 = 660\ \mu$J for the second step. The spot size of the laser beams in front of the filament was about 125 mm^2.

Figure 6 presents typical α-energy spectra obtained with the measurement sequence described above. The upper α spectrum includes 32 782 ^{155}Yb decays, accumulated over a collection time of 100 s with the lasers in resonance at a repetition rate of 250 Hz and a primary ^{52}Cr beam current of 0.8 pμA. The comparison with the lower spectrum, which was taken under the same conditions except that the lasers were off, results in a ^{155}Yb activity over background ratio of >116. The residual background in the lower spectrum is mostly due to non-resonant surface ionization.

Furthermore, laser scans were performed for both excitation steps. For this, data like the one shown in Figure 6 were taken for different laser frequencies. By plotting the number of ^{155}Yb α-decay events as a function of laser detuning, resonance lines with widths of 24 GHz for the first step and 21 GHz for the second step were found. Resonance enhancement factors between 20 and 30 were observed. This result demonstrates that the detection of atomic levels in fusion products from SHIP with the RADRIS method is possible.

The efficiency for resonance ionization is defined by the number of α decays n_α^{RIS}, counted with the PIPS detector, divided by the number n_{Yb} of ^{155}Yb fusion product ions produced in the target, both normalized to the number of

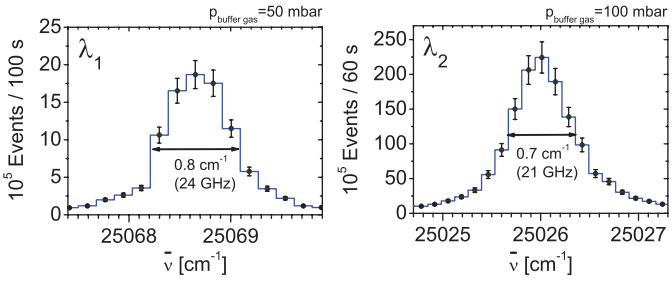

Fig. 7. Atomic resonance lines of a two-step excitation scheme in ^{155}Yb. First excitation step: $\lambda_1 = 398.9$ nm (left), second excitation step: $\lambda_2 = 399.6$ nm (right). The linewidths of more than 20 GHz can be attributed to pressure broadening and in the case of λ_1 also to saturation broadening which reveals itself in an emerging flat-top profile.

incoming ^{52}Cr projectiles n_p:

$$\epsilon_{RIS}^{tot} = \frac{n_\alpha^{RIS}/n_p}{n_{\mathrm{Yb}}/n_p}. \tag{2}$$

The denominator is the target fusion probability $n_{\mathrm{Yb}}/n_p = 8.6 \times 10^{-8}$, see equation (1) in Section 3 with $\epsilon_{SHIP} = 0.5$. The nominator has been determined from the dead time corrected α-count number $n_\alpha^{RIS} = 32\,782 \times 1.28 = 4.2 \times 10^4$ taken in a measuring time of 100 s and the number $n_p = 6.0 \times 10^{13}$. The latter was determined from the ^{52}Cr beam current of 10 μA at charge state 13+ measured with a Faraday cup for the measurement shown in Figure 6. In addition, the ^{52}Cr-beam duty cycle 5/20 and the experimental duty cycle 3/6, see Figure 5, were taken into account. From those parameters a total RIS efficiency of

$$\epsilon_{RIS}^{tot} = 0.8\% \tag{3}$$

has been calculated.

The total efficiency ϵ_{RIS}^{tot} can be factorized according to

$$\begin{aligned}\epsilon_{RIS}^{tot} &= \epsilon_{SHIP}\times\epsilon_{in}\times\epsilon_{stop}\times\epsilon_{ion}\times\epsilon_{det}\times\epsilon_N\times\epsilon_{evap}\times\epsilon_{RIS} \\ &= 0.5\times0.7\times0.8\times0.85\times0.36\times0.59\times\epsilon_{evap}\times\epsilon_{RIS} \\ &= 0.051\epsilon_{evap}\epsilon_{RIS},\end{aligned} \tag{4}$$

with the following sub-efficiency:

1. $\epsilon_{SHIP} \cong 0.5$, transmission efficiency of SHIP;
2. $\epsilon_{in} \cong 0.7$, transmission of ^{155}Yb ions through the entrance window;
3. $\epsilon_{stop} \cong 0.8$, stopping efficiency of ^{155}Yb ions in the buffer gas cell;
4. $\epsilon_{ion} = 0.85$, ionized fraction of stopped fusion products;
5. $\epsilon_{det} = \epsilon_\alpha\epsilon_\Omega = 0.36$, α-decay detection efficiency, with the α-decay probability $\epsilon_\alpha = 0.9$ and the solid angle ratio $\epsilon_\Omega = 0.4$;
6. $$\epsilon_N = \frac{t_{1/2}}{T\ln 2}(1 - e^{\frac{-T\ln 2}{t_{1/2}}}) = 0.59, \tag{5}$$
   part of the in $T = 3$ s on the catcher filament accumulated and not yet decayed ^{155}Yb atoms ($t_{1/2} = 1.75$ s);
7. ϵ_{evap}, probability of evaporation from catcher filament;
8. ϵ_{RIS}, probability of resonance ionization.

The conclusion is, since the total RIS efficiency is $\epsilon_{RIS}^{tot} \cong 0.008$, that the combined efficiency $\epsilon_{evap}\epsilon_{RIS} = 0.16$ is responsible for the biggest losses. Further improvements should focus on this part of the experimental procedure. These may include the question of molecule evaporation in context with improved gas purification. Additionally, losses of efficiency can occur during the evaporation of atoms from the catcher filament. The pulsed heating of the filament produces turbulences and updrafts in the buffer gas. Therefore, it is advantageous to place as many laser shots as possible within the the few hundred milliseconds of the evaporation process before the atoms are flushed out of the interaction volume with the laser beams. The ionization efficiency could be improved by 40% by increasing the repetition rate from 100 to 250 Hz. Higher repetition rates were not feasible with the available pump laser systems because they are associated with significant losses in laser power.

6 Outlook

The next step will be the search for atomic levels in ^{254}No. The nuclear reaction ^{208}Pb(^{48}Ca, $2n$)^{254}No at a beam energy of 216 MeV will be chosen. The recoil energy of the ^{254}No fusion products amounts to 40.5 MeV. It nearly coincides with the energy of 42.8 MeV of ^{152,153}Er recoils produced with the reaction ^{116}Sn(^{40}Ar, xn) ^{152,153}Er. For the latter the stopping distribution in the buffer gas cell was measured, see Figure 2.

For this experiment the measurement sequence will stay basically the same, with minor adjustments for the half-life of ^{254}No. The evaporation of nobelium from a tantalum surface is expected to work at least as well as the evaporation of ytterbium. A study of desorption enthalpies of actinides [20] states that nobelium should be desorbed as atoms at even lower temperatures than ytterbium. This is also consistent with observations on the evaporation of fermium from a tantalum-titanium sandwich filament [14]. However, the first step will be to determine the exact evaporation temperature of nobelium in the buffer gas with an experiment similar to the one described in Section 4.

The laser ionization of ^{254}No will also be accomplished in two steps. The first step will be provided by a tunable laser. Available for this experiment are an optical-parametric oscillator (OPO) and dye lasers which will be scanned in search for a resonance. The ionization step has to be non-resonant, using Nd:YAG or Excimer lasers. Their high pulse energies in the range of 60–300 mJ should be sufficient to compensate for the resonance enhancement of a Rydberg state excited with pulse energies of less than 1 mJ. The feasibility of non-resonant ionization has already been proven with the ionization of ^{255}Fm [21]. An important boundary condition for this approach is that the combined photon energies of the two excitation steps have to be larger than the ionization energy, which has yet to be determined for nobelium. Hartree-Fock calculations [22], extrapolations from lanthanides [23] and from

the experimentally determined ionization energies of other actinides [24] place the ionization energy of nobelium between 52 800 cm^{-1} and 54 000 cm^{-1}.

By analogy with ytterbium, low lying $5f^{14}7s7p\ ^1P_1$ and $5f^{14}7s7p\ ^3P_1$ terms are also expected for nobelium. Their excitation energies were recently calculated with both, a MCDF [25] and an intermediate Hamiltonian coupled cluster method [26]. The MCDF method predicts the $^3P_1$ state at 20 945 cm^{-1} and the coupled cluster method at 20 484 cm^{-1}. Even within the limits of the rather large uncertainties of several hundred cm^{-1} of these calculations, it seems to be rather unlikely to reach the estimated ionization limit from the $^3P_1$ level with the wavelengths of the available pump laser systems of 308 nm, 351 nm, and 355 nm. Better suited seems to be the $^1P_1$ term which is predicted by MCDF and coupled cluster methods at 27 070 cm^{-1} and 30 108 cm^{-1}, respectively. High transition rates into the ground state of $A_{ki} = 5 \times 10^8\ s^{-1}$ are predicted for this level by the coupled cluster model [27]. From these calculations, including their limited accuracy, an estimated scan range from about 26 000 to about 31 000 cm^{-1} seems to be appropriate to find the level. The beams can be provided with dye lasers and the OPO system as well. The photon energy of the available pump lasers is very likely high enough to exceed the ionization limit.

With a ^{254}No production rate of 17/s in the target and an overall efficiency of 0.8% one would expect to detect 0.14 events/s at resonance. A long range dye laser scan would cover 24 cm^{-1}/h if a bandwidth of ≈0.2 cm^{-1}, and a measurement time of 30 s per step is assumed. A long range OPO scan would cover 96 cm^{-1}/h. On the one hand its bandwidth of ≈4 cm^{-1} is much broader, on the other hand the measurement time must be increased by a factor of 5 to 150 s per step since the efficiency of resonance ionization is reduced due to the limited repetition rate of 50 Hz of the OPO system. Therefore, the OPO laser system would be preferable for the level search, while the dye laser system would be useful for precision measurements like the determination of exact level energies, line widths and transition rates once the level has been found.

If the search for the $^1P_1$ term would be successful the next step could be to find the ionization limit by scanning with a tunable laser across the ionization threshold. Corrections for pressure shifts would be necessary but it would nevertheless be an important reference point for valence-shell computations and further more precise experiments on nobelium.

7 Conclusions

The application of the RADRIS method, optimized for on-line spectroscopy on fusion products of the SHIP facility at GSI, has been demonstrated with the resonant ionization of the α active ^{155}Yb atoms in a two-step excitation scheme. The first step was a transition from the $4f^{14}6s^2\ ^1S_0$ ground state to the $4f^{14}6s6p\ ^1P_1$ term, the second step the excitation of a Rydberg state close to the ionization limit from which the electron is excited into the continuum by buffer gas collisions. A novel method with high efficiency was developed in which the ionized fraction of the ^{155}Yb fusion product beam from SHIP, stopped in the argon buffer gas, was collected onto a catcher filament from which the radioactive species were re-evaporated as atoms. The atoms were resonantly ionized with laser beams and the ions subsequently transported by electrical fields to a semiconductor PIPS detector which detects the resonance ionization by the α decay of ^{155}Yb. This method yielded significant efficiency gains compared with earlier attempts to perform resonance ionization directly on the neutral part of the stopped fusion products. The reason is that the larger ion fraction of about 85% of the thermalized ^{155}Yb can be utilized as well as that the re-evaporated atoms remain concentrated in a rather small volume. The latter fact increased the interaction efficiency with the laser beams dramatically. In order to simulate the search for atomic levels, laser scans over the known levels in ^{155}Yb were performed. The overall experimental efficiency was determined to be nearly 1%. Even without further improvements — which seem to be possible — this efficiency is already sufficient for the atomic level search in nobelium.

We would like to thank H.J. Kluge for fruitful discussions and Ch. Rauth for his active support during the course of the experiment at GSI. This work was supported by the Bundesministerium für Bildung und Forschung under contract No. 06 MZ 169I.

References

1. M. Schädel, Angewandte Chemie-International Edition **45**, 368 (2006)
2. A. Türler, Eur. Phys. J. A **15**, 271 (2002)
3. H.W. Gäggeler, Eur. Phys. J. A **25**, 583 (2005), Suppl. 1
4. R. Eichler et al., Radiochimica Acta **94**, 181 (2006)
5. C.E. Düllmann et al., Nature **418**, 859 (2002)
6. H.W. Gäggeler, *Confirmation of the decay of* ^{283}112 *and evidence for a behaviour of element 112 as a volatile metal*, in *Workshop on the Atomic Properties of the Heaviest Elements* (2006), `http://www.ha.physik.uni-muenchen.de/heaviest_atoms/`
7. V.G. Pershina, Chem. Rev. **96**, 1977 (1996)
8. B. Fricke, E. Johnson, G. Rivera, Spectrochimica Acta **62**, 17 (1993)
9. W.C. Martin, J. Sugar, Phys. Rev. A **53**, 1911 (1996)
10. E. Eliav, U. Kaldor, Y. Ishikawa, Phys. Rev. Lett. **74**, 1079 (1995)
11. W. Lauth, H. Backe, M. Dahlinger, I. Klaft, P. Schwamb, G. Schwickert, N. Trautmann, U. Othmer, Phys. Rev. Lett. **68**, 1675 (1992)
12. H. Backe et al., Phys. Rev. Lett. **80**, 920 (1998)
13. H. Backe, A. Dretzke, M. Hies, G. Kube, H. Kunz, W. Lauth, M. Sewtz, N. Trautmann, R. Repnow, H.J. Maier, Hyperfine Interact. **127**, 35 (2000)
14. M. Sewtz et al., Phys. Rev. Lett. **90**, 163002 (2003)

15. H. Backe et al., Nucl. Instrum. Meth. Phys. Res. B **126**, 406 (1997)
16. H. Backe, A. Dretzke, S. Fritzsche, R.G. Haire, P. Kunz, W. Lauth, M. Sewtz, N. Trautmann, Hyperfine Interact. **162**, 3 (2005)
17. M. Leino et al., Eur. Phys. J. A **6**, 63 (1999)
18. H. Backe, W. Lauth, W. Achenbach, M. Hain, A. Scherer, A. Steinhof, S. Tölg, S. Ziegler, Nucl. Instrum. Meth. Phys. Res. B **70**, 521 (1992)
19. W. Reisdorf, Z. Phys. A **300**, 227 (1981)
20. B. Eichler, S. Hübener, N. Erdmann, K. Eberhard, H. Funk, G. Hermann, S. Köhler, N. Trautmann, G. Passler, F. Urban, Radiochim. Acta **79**, 221 (1997)
21. M. Sewtz et al., Spectrochim. Acta B **58**, 1077 (2003)
22. K. Rajnak, B. Shore, J. Opt. Soc. Am. **68**, 360 (1978)
23. J. Sugar, J. Chem. Phys. **60**, 4103 (1974)
24. N. Erdmann et al., J. Alloys Comp. **271**, 837 (1998)
25. S. Fritzsche, Eur. Phys. J. D **33**, 15 (2005)
26. A. Borschevsky, E. Eliav, M. Vilkas, Y. Ishikawa, U. Kaldor, *Transition energies of Yb, Lu, No, and Lr by the intermediate Hamiltonian coupled cluster method*, in *Workshop on the Atomic Properties of the Heaviest Elements* (2006), `http://www.ha.physik.uni-muenchen.de/heaviest_atoms/`
27. U. Kaldor, private communication, 2006